Acta Geophysica (2024) 72:2071–2081
https://doi.org/10.1007/s11600-023-01141-1

RESEARCH ARTICLE - HYDROLOGY AND HYDRAULICS

Influence of biochar on the water permeability of compacted clay subjected to freezing–thawing cycles

Zhongkui Chen[1] · Viroon Kamchoom[2] · Anthony Kwan Leung[3] · Jiaxiang Xue[4] · Rui Chen[4,5]

Received: 18 April 2023 / Accepted: 21 June 2023 / Published online: 13 July 2023

Abstract

Seasonal variation of soil surface temperature, such as freezing and thawing, can induce increases in the water permeability in clay by mobilizing clay pore structure. This kind of weather-induced change in clay behavior may worsen the water-sealing performance during the construction and after closure operation of engineered structures such as soil barriers for tailings or man-made slopes. There is limited knowledge towards the influence of freezing–thawing cycles on clay microstructure and saturated permeability (K_{sat}). This study investigated the saturated permeability of clay under freezing–thawing cycles and explored the uses of biochar as eco-friendly amendment to manipulate the permeability of compacted clay. Clay specimens were compacted with different initial water contents (30%, 34%, and 38%). The biochar application rates of 0%, 2%, 4%, 8% (by dry weight) were applied to measure their effects on the permeability of clay specimens. Saturated permeability was measured by the falling head tests. Any variation of biochar amended clay microstructure after freezing–thawing cycles was captured by the scanning electron microscope. The K_{sat} was reduced by about one order of magnitude when the biochar application rate was larger than 4%. This may be attributed to the increase in the filling of the biochar particles in the clay intra-aggregate pores upon the transport of liquid water during the repeated freezing–thawing processes. The biochar may thus be recommended to minimize the K_{sat} of geo-environmental structures in cold regions when sufficiently large application rate was used to facilitate the pore-filling process.

Keywords Freezing–thawing · Biochar · Saturated permeability · Compacted clay

Introduction

Compacted clays in cold regions undergo cyclic freezing–thawing process, causing an increase of macroscopic parameter due to shrinkage cracks during freeze–thaw process and large pores that are left after ice crystal thawing, and hence an increase in clay permeability (K_s) (Tang and Yan 2015). In fact, saturated permeability (K_{sat}) is one of the most crucial hydraulic parameters in determining the seepage and stability of clay barriers in many civil engineered structures such as man-made slopes, compacted embankments, tailings dams and buried gas pipelines. Freezing–thawing cycles pose high risk to the degradation of these structures by increasing K_{sat} associated with the resultant increase of water infiltration and percolation in these systems (Shibi and Kamei 2014; Huang et al. 2021; Chen et al. 2022; Garg et al. 2022; Kalkan et al. 2022). Therefore, the clay improvement is needed to manipulate the integrity and functionality of these afore-mentioned systems. In general, the conventional clay amendments, such as fly ash

Edited by Dr. Ankit Garg (ASSOCIATE EDITOR).

✉ Rui Chen
chenrui1005@hotmail.com

[1] Shenzhen Yanzhi Science and Technology Co Ltd, Shenzhen 518101, China

[2] Excellent Centre for Green and Sustainable Infrastructure, Department of Civil Engineering, School of Engineering, King Mongkut's Institute of Technology Ladkrabang, Bangkok 10520, Thailand

[3] Department of Civil and Environmental Engineering, The Hong Kong University of Science and Technology, Hong Kong SAR, People's Republic of China

[4] School of Civil and Environmental Engineering, Harbin Institute of Technology Shenzhen (HIT Campus), University Town of Shenzhen, Xili, Shenzhen 518055, China

[5] Guangdong Provincial Key Laboratory of Intelligent and Resilient Structures for Civil Engineering, Shenzhen 518055, China

and lime, were used to reduce K_{sat} in permafrost regions. However, the presence of both fly ash and lime are highly alkaline and thus provide negative impacts to the urban environment (Chen et al. 2016; Palmer et al. 2000). Compared to the conventional amendments, biochar is a promising alternative amendment for restoration of ecological environment because most of them are neutral or slightly alkaline in pH (Lehmann and Joseph 2009; Bordoloi et al. 2019) and can reduce greenhouse gas emission (Chiu and Huang 2020; Garg et al. 2021). Biochar addition is suitable for crop growth that can increase agricultural products or enhance root reinforcement for engineering slopes (Hussain et al. 2020; Chen et al. 2023a, b). It is also helpful for the improvement of physico-chemical properties, such as increasing pH, exchangeable K, Ca and Mg and cation exchange capacity of farmlands (Uzoma et al. 2011; Al-Wabel et al. 2017).

However, past studies have not yet come to a consistent conclusion on the influence of biochar on the K_{sat} of amended mixture. Wong et al. (2018) concluded that the K_{sat} of clay increases with the increase of peanut shell biochar (produced by slow pyrolysis method at 500 °C for 30 min) application rate due to the shift of the dominant clay pore diameter from mesopores to macropores. However, some scholars found that the saturated permeability of biochar amended soil decreases with the increase of biochar application rate. For instance, Githinji (2014) concluded that as the increase of peanut hulls (*Arachis hypogaea*) biochar application rate, the K_{sat} of the loamy sand decreased significantly due to the hydrophobicity of the organic matter present in biochar amendment. Brockhoff et al. (2010) reported a decrease in K_{sat} for sand-based turfgrass root zones with the increase of switchgrass (*Panicum virgatum*) biochar application rate. The discrepancy may be due to the differences in biochar feedstock types and characteristics such as pyrolysis temperature and particle size used in these studies. Indeed, Liu et al. (2018) evaluated four types of biochar (pine, mesquite, miscanthus, and pelletized sewage waste) subjected to several freezing–thawing cycles and found that the grain size of all the biochars except the sewage waste biochar decreased with the increase of freezing–thawing cycles. They attributed this difference to the feedstock of the sewage waste biochar which is not dominated by plant material.

Although past studies focused on many influencing factors of biochar addition on clay K_{sat}, there are rare studies on the influence of freezing–thawing cycle on the K_{sat} of biochar amended clay. Fu et al. (2019) investigated the change of K_{sat} of corn straw biochar amended loam collected from different depths of loam layers subjected a freezing–thawing period in a field experiment conducted in idle farmland (agricultural soil). They found that the K_{sat} of different layers decreased with increases in biochar application rate due to the blockage of loam pores by the biochar fine particles. However, agricultural soils normally had lower degree of compaction aiming to provide adequate air and nutrient transport to support crop growth. Furthermore, as the initial conditions in field experiments such as compaction water content, freezing–thawing cycle and the temperature during freezing–thawing cycles are hard to control, it is difficult to capture the variations of permeability of biochar-amended material in the field. Comparatively, high compaction degree is often required in geotechnical infrastructures such as man-made slopes and compacted embankments (Chen et al. 2021, 2023a, b; Wang et al. 2023). This study focuses on engineered soils which are normally compacted at a much higher degree of compaction to reduce soil permeability. Thus, the objective of this study is to investigate the saturated permeability (K_{sat}) of a highly compacted clay under freezing–thawing cycles in a well-controlled condition. This study also explored potential engineering uses of biochar with different application rates and initial compaction water contents to manipulate the K_{sat} of compacted clay. The K_{sat} of each test was determined through a series of falling head permeability tests. Any change of the microstructure of biochar amended clay (BAC) after the freezing–thawing cycles were explored by scanning electron microscope (SEM). Findings from this study would dictate the efficient use of biochar for soil systems in cold regions.

Materials and methods

Test scheme

Four series of laboratory tests, comprising altogether 68 specimens, were carried out to measure and compare the saturated permeability (K_{sat}) of clay amended with different application rates of biochar and subjected to different numbers of freezing–thawing cycles. The four series were named as BC0, BC2, BC4 and BC8 according to the four biochar application rate (defined as dry weight of biochar/dry clay mass B = 0%, 2%, 4% and 8%) respectively. Each of the test series consisted of 17 BAC specimens, 15 of which considered three initial compacted water contents (CWC) (i.e. 30%, 34% and 38% at the same dry density of 1.17 g cm^{-3} (i.e., corresponding to 90% of the maximum dry density of B0 specimens)) and five different cycle numbers (i.e., N = 0, 1, 3, 8 and 12 cycles). The remaining two specimens that were compacted to the optimum water content and subjected to 0 and 12 cycles of freezing–thawing were used to measure the BAC microstructure via SEM. Compacted clays in the first test series are untreated specimens, whereas the other three series of tests used the treated BAC specimens with biochar application rate of 2%, 4% and 8%. Table 1 summarises the details of the four test series.

Table 1 Test scheme

Test series ID	Biochar application rate, B (%)	Initial compaction water content, CWC (%)	Number of freeze–thaw cycle, N	Number of BAC specimens for permeability test	Number of BAC specimens for SEM test
BC0	0	30 34 38	0 1 3 8	15	1
			12		1
BC2	2	30 34 38	0 1 3 8	15	1
			12		1
BC4	4	30 34 38	0 1 3 8	15	1
			12		1
BC8	8	30 34 38	0 1 3 8	15	1
			12		1

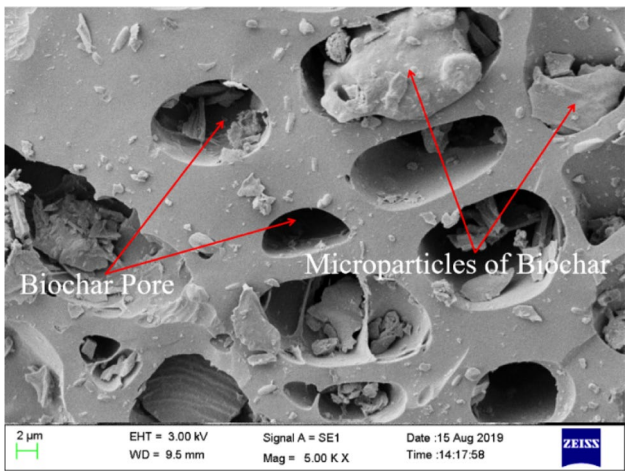

Fig. 1 SEM image (×5000) of biochar

Test materials and sample preparation

The biochar used in this study was purchased from a recycled material company in China. It was pyrolysed from peanut shells under anaerobic conditions at 500 °C for one hour. The natural water content and organic matter of the biochar are 4.9% and 30.2%, respectively. As indicated by the SEM image (×5000) in Fig. 1, the peanut shell-derived biochar has a honeycomb-like microstructure, characterized by low specific gravity (i.e. 2.07; Table 2), small pore volume and average pore diameter but large surface area (Chen et al. 2020). Any impurities and peanut shell that had not been completely pyrolysed and had a diameter larger than 0.5 mm were sieved prior to the use of clay amendment.

Table 2 Basic physical parameters of testing materials

	Liquid limit (%)	Plastic limit (%)	Specific gravity
B0	78.5	31.6	2.66
B2	82.6	32.5	2.61
B4	83.1	33.7	2.54
B8	85.9	35.3	2.44
Biochar	–	–	2.07

B0, B2, B4, and B8 represent 0%, 2%, 4%, and 8% of biochar application rate, respectively

The clay used in the test was commercial kaolin clay. The basic physical properties of the clay were determined in accordance with the standard GB/T 50123–2019 of China. Some index properties of the test soil are summarised in Table 3. Figure 2a shows the particle size distributions (PSDs) of the biochar and the clays amended with different application rates of biochar. As expected, the addition of biochar made the clay coarser. The PSDs of the different BACs were similar. Figure 2b shows the compaction curves of the biochar-amended clays. Increasing the application rates (from 0 to 8%) of biochar resulted in a reduction in the maximum dry density (from 1.3 to 1.2 g cm^{-3}) because the biochar particles have lower specific gravity (i.e. 2.07), compared with the clay (i.e. 2.66). The addition of biochar also accompanied an increase in the optimum water content (from 34 to 36%) due to the continued improvement of the water holding ability of clay by the biochar. The addition of biochar enhanced the liquid limit and plastic limit of the clay (Table 2) because biochar particles are more plastic as compared with clay particles. Dry clay powder was first mixed with dry biochar at the designated application rates (Fig. 3a and b). Then the mixture was mixed with water to achieve the targeted gravimetric water content (30%, 34% and 38%, denoted as W30, W34 and W38, respectively) (Fig. 3c). The moist BAC mixture was kept in a sealed plastic bag for 24 h for moisture equilibrium. Then, the BAC mixture was compacted in a stainless-steel cutting ring with an inner diameter of 61.8 mm and a height of 40 mm (Fig. 3d). Note that we compacted all the soil specimens at the same dry density (1.17 g cm^{-3}) and the same as-compacted water content.

Table 3 Index properties of the clay soil tested in this study

Property	Value
Specific gravity	2.66
Liquid limit (%)	78.5
Plastic limit (%)	31.6
Plasticity Index (%)	46.9
Maximum dry density (g cm^{-3})	1.3
Optimum water content (%)	34
CEC (mmol/g)	0.05
Main mineral composition	Kaolinite
Chemical component	SiO_2-52.41%
	Fe_2O_3-0.6%
	Al_2O_3-43.08%

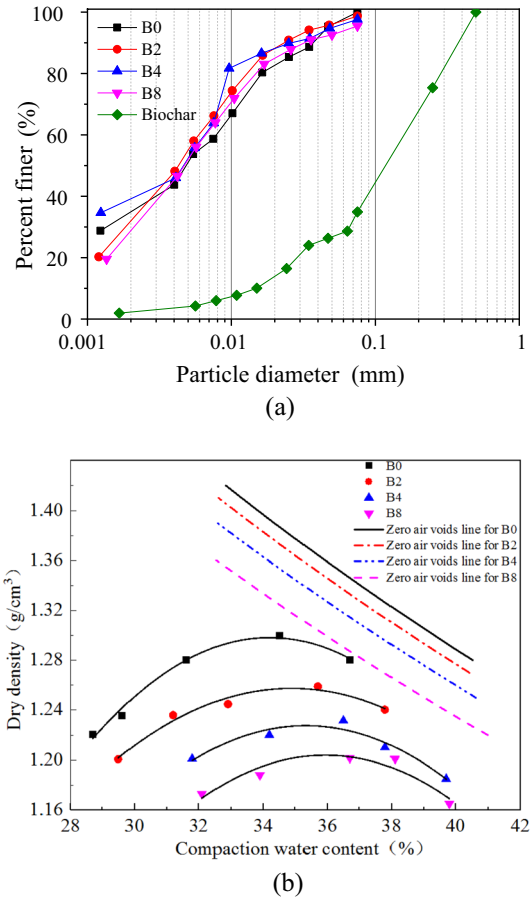

Fig. 2 Basic physical properties of the BAC: **a** particle size distribution; **b** compaction curve (B0, B2, B4, and B8 represent 0%, 2%, 4%, and 8% of biochar application rate, respectively)

This means that the compaction efforts used to produce these specimens were different. The water contents, 30%, 34% and 38%, should not be referenced to the standard proctor compaction curve shown in Fig. 2b where the same compaction effort was used.

Test procedure for BAC freezing and thawing

After moisture equilibrium, all 60 samples were placed in a temperature and humidity control chamber (model: CK-800G; China) for simulating controlled freezing–thawing cycles (see Fig. 4). The freezing–thawing process of the soil specimens was conducted following the ASTM standard (ASTM D6035/D6035M-13 2013). Each sample was wrapped with a plastic film to prevent moisture loss from the sample to the air in the test chamber. The range of air temperature controlled by the chamber was from − 60 °C to 150 °C with an accuracy of ± 0.1 °C. Based on the review of past freeze-thawing experiments reported by Dong and Chen (2017), the strength of soil would reach a stable value when the freezing temperature is below − 10 °C. Therefore, a freezing temperature of − 15 °C and a thawing temperature of 20 °C were set to introduce freezing and thawing to the samples. After each of the target temperature (i.e. − 15 and 20 °C) was reached, the samples were left in the chamber for 12 h, which were deemed sufficiently long for the clay to have been completely frozen or thawed, according to pilot tests and the review reported by Dong and Chen (2017). The samples were subjected to 0, 1, 3, 8 and 12 freezing–thawing cycles. When the designated cycle number has been reached, the samples were taken out from the chamber and used to conduct permeability and SEM tests.

Measurement of saturated permeability

Saturated permeability (K_{sat}) of the samples were measured by a permeameter (Model TST-55) which adopts the falling head testing method, following the standard GB/T 50123–2019. The top and bottom of each sample was covered with a piece of filter paper, and a porous stone was then placed on the filter paper at each end. The samples were then water-saturated by the vacuum saturation method described in the ASTM standard (ASTM C1202 2006). The setup of the falling head permeability tests is depicted in Fig. 5. In this method, the sample was first placed in a vacuum container for 3 h without water and de-aerated water was then introduced into the container until all the samples were submerged for 8 h.

Microstructure analysis

After subjecting to freezing–thawing cycles, a total of 8 samples taken out from the chamber were trimmed to extract small cubes of approximately $10 \times 10 \times 10$ mm^3

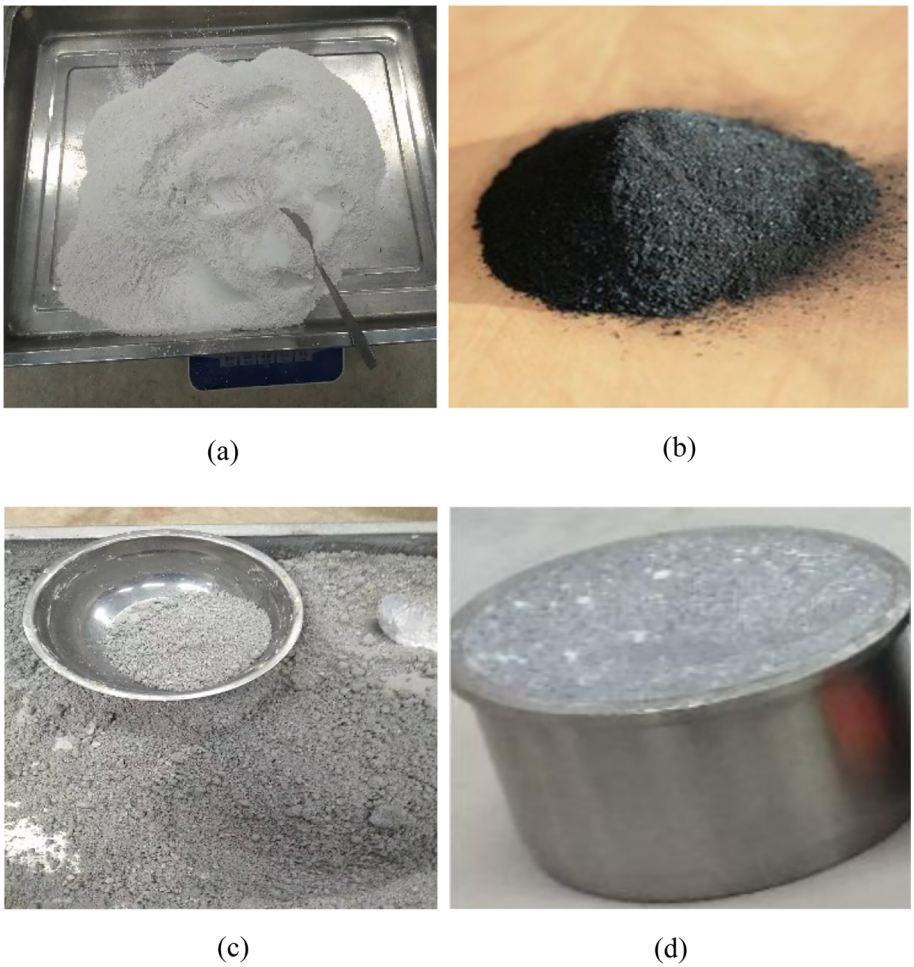

Fig. 3 The images of soil preparation: **a** dry clay powder; **b** dry biochar powder; **c** wet mixture of clay and biochar; **d** compacted soil specimen

from the middle part of the samples. Prior to the SEM test, the subsample cubes were pretreated in liquid nitrogen at − 195 °C for 5 min and then placed in a vacuum freeze-dryer (− 40 °C) for 48 h. Indeed, Ma (2014) has demonstrated that the freeze-drying procedure causes minimum fabric changes on clay. Finally, an open-source software, *ImageJ*, was used to analyse and interpret the SEM images for quantifying the dimension of BAC pores and any micro-crack width introduced by the freezing–thawing cycles.

Statistical analyses

The measured K_{sat} were assessed for normality using the skewness and kurtosis. When the skewness absolute value is less than 3 and the kurtosis absolute value is less than 10, the data is deemed to conform to normal distribution. Three-way analysis of variance (ANOVA) with Tukey HSD post hoc tests were conducted to analyze the differences of K_{sat} with the following factors: (i) biochar application rate (B = 0, 2, 4, and 8%), (ii) compaction water content (CWC = 30, 34 and 38%), and (iii) number of freezing–thawing cycle (N = 0, 1, 3, 8 and 12). All the statistical analyses were carried out by SPSS 24.0 (SPSS Inc., Chicago, IL). The test results were presented as mean ± standard deviation (SD) in figures.

Results and discussion

Effects of freezing–thawing cycles and biochar application rate

Figure 6 shows the variations of K_{sat} of untreated clay with freezing–thawing cycles at different compaction water contents (30%, 34% and 38%). The K_{sat} increased exponentially with the number of cycles. The increase was more than one order of magnitude during eight cycles, beyond which the change in K_{sat} was minimal (i.e., within ± 10%). It can also be seen that higher as-compacted water content led to greater K_{sat}. The results of both ANOVA (Table 4, $p = 0.000$) and Tukey HSD (Table 5, $F = 13.903$, $p < 0.0001$) consistently suggest that the observed increase was significant. The findings are similar to the results of compacted clay

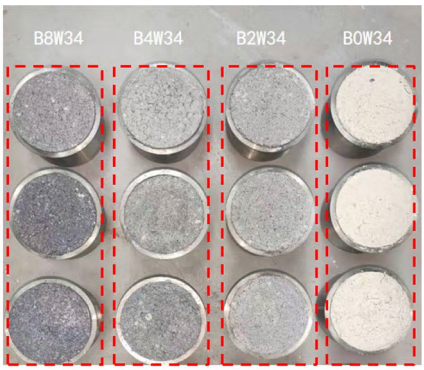

(a) BAC specimens before freezing-thawing

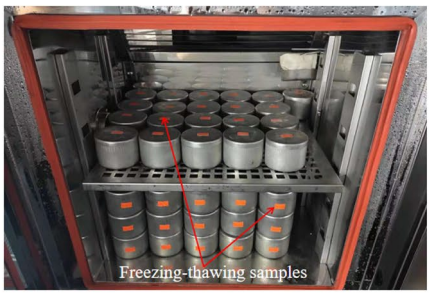

(b) Setup of the BAC specimens in the interior of chamber

(c) Photography of the controller of the temperature and humidity chamber

Fig. 4 Arrangement of the BAC specimens in the temperature and humidity control chamber

reported by Othman and Benson (1993). As the number of freezing–thawing cycles increases, the repeated appearance and disappearance of ice lenses formed within the BAC pore space would induce more micro-cracks and hence more permeable to water. However, after eight cycles of

Fig. 5 The setup of the falling head permeability test

freezing–thawing process, the number of new ice lenses may become negligible and hence further increases in K_{sat} cease.

Figure 7 shows the variations of K_{sat} with the biochar application rate at different numbers of freezing–thawing cycles at the same optimum compaction water content of 34%. It is interesting to see that before subjecting to any freeze/thaw cycle (i.e. N0), the biochar application of less than 4% did not introduce noticeable change to K_{sat} but when the application rate was increased to 8%, there was a significant drop of K_{sat} by one order of magnitude. This maybe because that at high biochar content (i.e., larger than 4%), the permeability of the BAC decreases with increasing biochar content due to the combined effect of clay aggregation and biochar inhibition in the water flow. Some of the clay inter-aggregate pores may be filled by the biochar particles as the application rate increased to a certain threshold (i.e., 8% in this study). However, at low biochar content (i.e.,

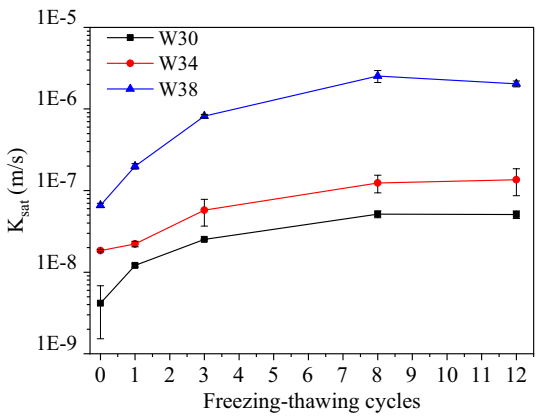

Fig. 6 Changes of saturated permeability with the number of freezing–thawing cycle for bare clay. Experimental data points are presented in mean ± standard deviation (SD). SD of each point of K_{sat} is shown by an error bar

Table 4 *F* and *p* values of the three-way ANOVA for the effects of biochar application rate (B), compaction water content (CWC), number of freezing–thawing cycle (N), and their interactions on the saturated permeability K_{sat} of clay and biochar-amended clay

Factor(s)	*F*	*p*
CWC	428.210	.000
N	152.899	.000
B	32.744	.000
CWC * N	99.582	.000
CWC * B	20.254	.000
N * B	7.996	.000
CWC * N * B	5.649	.000

B, biochar application rate; CWC, compaction water content; N, number of freezing–thawing cycle. Values in bold represent statistical significance at probability level 0.05

Table 5 Tukey post hoc test results

Factors	*F*	Order of significance
B	2.977*	B8 < B0 < B4 < B2
CWC	38.937***	W30 < W34 < W38
N	13.903***	N0 < N1 < N3 < N8 < N12

B, biochar application rate; CWC, compaction water content; N, number of freezing–thawing cycle

*$p < 0.05$; ***$p < 0.0001$

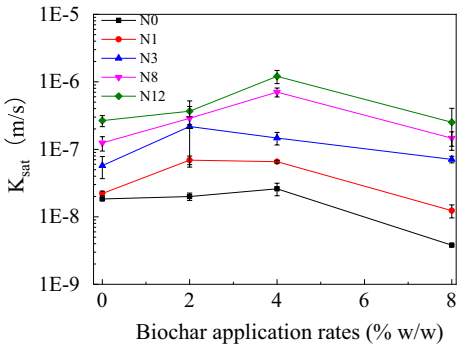

Fig. 7 Influence of biochar application rate on saturated permeability at different freezing–thawing cycles for specimens compacted at optimum water content of 34%. Experimental data points are presented in mean ± standard deviation (SD). SD of each point of K_{sat} is shown by an error bar

smaller than 4%), the effect of biochar incorporation on permeability is negligible because it no longer acts as a filling material to retard water flow. After freezing–thawing cycles, the biochar, irrespective to the application rate, improved the K_{sat} due to the formation of micro-cracks and continued increase in their size. The improvement is more significant when the biochar application rate is in the range of 2~4%. When the biochar application rate is low (i.e., < 4%), the presence of biochar may increase the seepage pathways in the clay and thus increases the K_{sat} since there are many open-pores in the biochar particles (Fig. 1). For instance, as the biochar application rate is less than 4%, the K_{sat} of BAC specimens was increased about 2 ~ 10 times, even with only one cycle of freezing–thawing. This may be due to the formation of micro-cracks induced by the freezing expansion and thawing subsidence which is similar to the bare clay case. For relatively larger application rate (i.e. 4 ~ 8%), K_{sat} decreased. This may be because some of the micro-cracks formed during the freezing–thawing process were filled by more biochar particles (fragments) as the biochar application rate increased to a certain amount (i.e., 8%). The wider the micro-cracks, the much easier for biochar and clay particles to fill. Lim et al. (2016) also observed the similar trend when adding biochar to loam without freezing–thawing. Note that K_{sat} of BAC is highly dependent on the pore structure of the biochar and the clay. As Barnes et al. (2014) pointed out, there are two water flow paths in biochar-amended clay. One path is through the inter-pore between biochar and clay, whereas the other is through the intra-pores within the biochar particles (Fig. 1) of which the size is larger than water molecules. Both water flow paths can promote more fine particles clogging the pores and hence reduce K_{sat}.

Volume change and microstructure of BAC under freezing–thawing

Figure 8 shows the measured volumetric strain of BAC sample (with initial water content of 34%) after subjecting to different numbers of freezing–thawing cycles. The figure demonstrates that the volumetric strain increased with the increase of number of cycles of freezing–thawing. This is because that as water freezes below 0 °C and transforms from liquid to solid state, the volume would increase by approximately 9% due to the opening of the lattice of its hexagonal crystal structure. More ice lens was formed as the cycles of freezing–thawing increased. For instance, the thickness of BAC with the biochar application rate of 8% is 40.0 mm, 40.5 mm, 41.9 mm, 43.5 mm, 43.6 mm after subjecting freezing–thawing cycle of 0, 1, 3, 8, 12, respectively. Hence, the corresponding void ratio was 1.131, 1.157, 1.232, 1.317 and 1.324. The increase in void ratio with the cycle number partially explains the increase in K_{sat}. Indeed, the results from statistical analyses confirmed that the number of freezing–thawing cycle has more influence on the K_{sat} than that of biochar application rate (Table 4, $F = 32.744$ for B, $F = 152.899$ for N, $p = 0.000$). Furthermore, the figure demonstrated that the increase of volumetric strain after eight cycles of freezing–thawing almost terminated. This indicated that freezing expansion and thawing subsidence effect resulted in the irreversible volume change of BAC and hence influence the K_{sat}. This is because when the ice crystals continue to increase under freezing condition, the

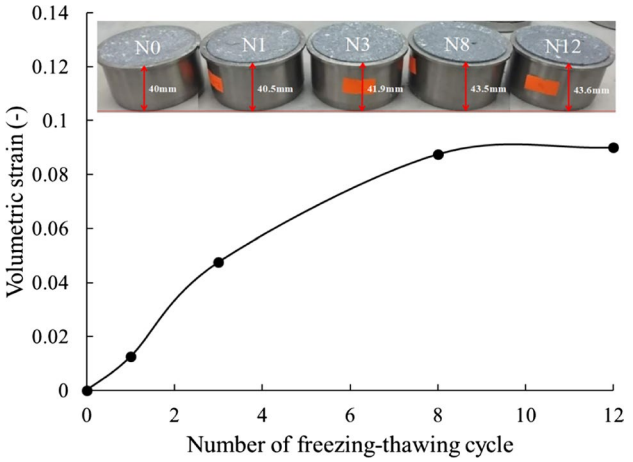

Fig. 8 Volume change of the BAC specimens (soil compaction water content is 34% and biochar application rates is 8%) subjected to different freezing–thawing cycles (soil thickness is 40.0 mm, 40.5 mm, 41.9 mm, 43.5 mm, 43.6 mm after freezing–thawing cycle of 0, 1, 3, 8, 12, respectively. N0, N1, N3, N8, N12 represents the number of freezing–thawing cycle)

interaction between ice crystals and BAC particles intensifies (Andersland and Anderson 1978). However, during the thawing period, part of ice lens formed in the freezing process was associated with water migration to the previous freezing zone and hence some segregational ices were developed (Azmatch et al. 2012).

Figure 9 shows the pore structure changes of BAC after 0 and 12 cycles of freezing–thawing. Before the samples were subjected to freezing–thawing, more pores were presented in the biochar particles (Fig. 9a and b). However, some clay particles were filled in the biochar pores for the 8% application rate (Fig. 9c) and hence reduced the K_{sat} of the BAC (Fig. 7). This further explained the increase of K_{sat} from 0 ~ 4% application rate but decrease after 4% is exceeded (Fig. 7).

Effects of as-compacted water contents

Figure 10 shows the variations of K_{sat} with as-compacted water content. For all the cases of BAC, the K_{sat} were increased as the as-compacted water content increased after cycles of freezing and thawing. For instance, the K_{sat} of B0 compacted with 38% water content was increased almost one order of magnitude (Fig. 10a). After the BAC specimens were subjected to cycles of freezing–thawing, the K_{sat} of B8 decreased as compared to B0. For instance, after one cycle of freezing–thawing, K_{sat} of B8 is decreased by 49.7%, 44.3%, 90.6% at 30%, 34%, 38% of compaction water content,

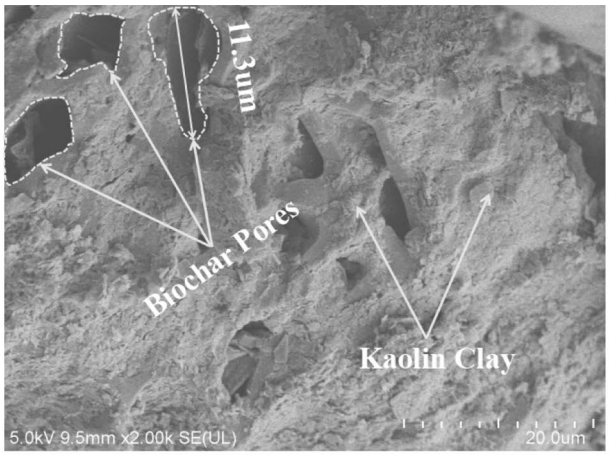

(a) B4N0

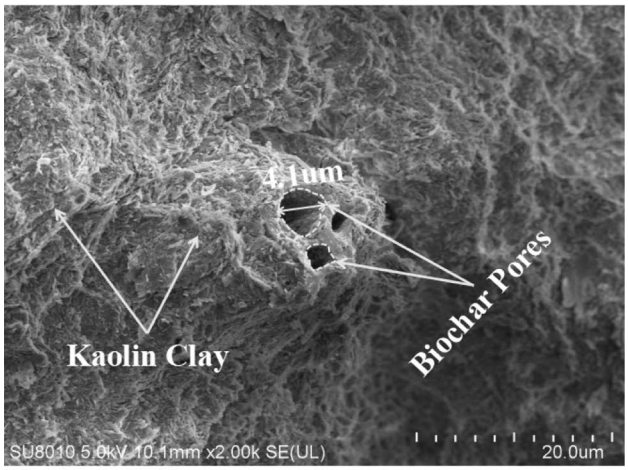

(b)B4N12

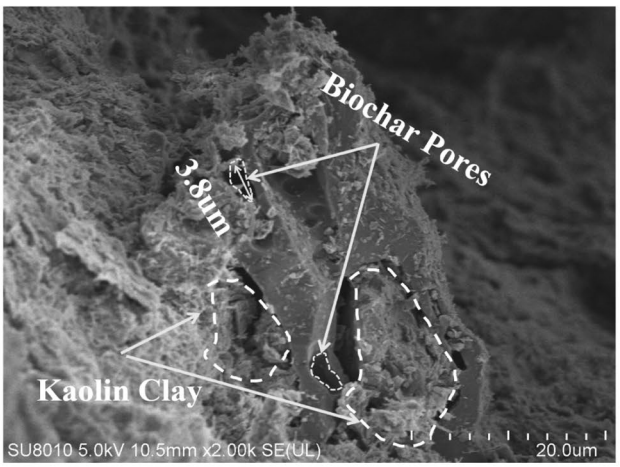

(c) B8N12

Fig. 9 Pore structure of BAC samples after 0 and 12 cycles of freezing–thawing

respectively (Fig. 10b). The three-way ANOVA results also show that the compaction water content has significant effect on K_{sat} (Tables 4 and 5, $p < 0.0001$). Furthermore, the Tukey HSD test results indicated the compaction water content is the most influencing factor on K_{sat} among the other three influencing factors (Table 5, $F = 38.937$, $p < 0.0001$). The results are expected as the compaction of BAC with different water contents would yield different pore structures, pore amounts and distributions (Wong et al. 2017), and thus more variations in K_{sat}. The experimental results confirmed that the increase in the compaction water content can increase the BAC expansion, resulting in a higher K_{sat}. After cycles of freezing and thawing, more compaction water content can provide higher K_{sat} of BAC specimens. Three-way ANOVA analysis results from the test of combined effects between compaction water content and number of freezing–thawing cycles also indicate significant effects on K_{sat} (Table 4, $p = 0.000$). The reason behind this mechanism is that there is more ice forming in BAC pores during freezing process for the BAC specimens with higher compaction water content. The liquid water can flow from unfrozen zone into the frozen zone in BAC specimens during the freeze–thaw process. When water freezes at the frost front, its original energy balance are destroyed. In order to maintain the energy of the phase change, unfrozen water migrates faster to achieve a new balance. Gu et al. (2016) found that under freezing–thawing condition, the larger the compaction water content is, the larger the water migration in loess. Therefore, when the compaction water content increases from 30 to 38% (Fig. 10), more water migration was required to

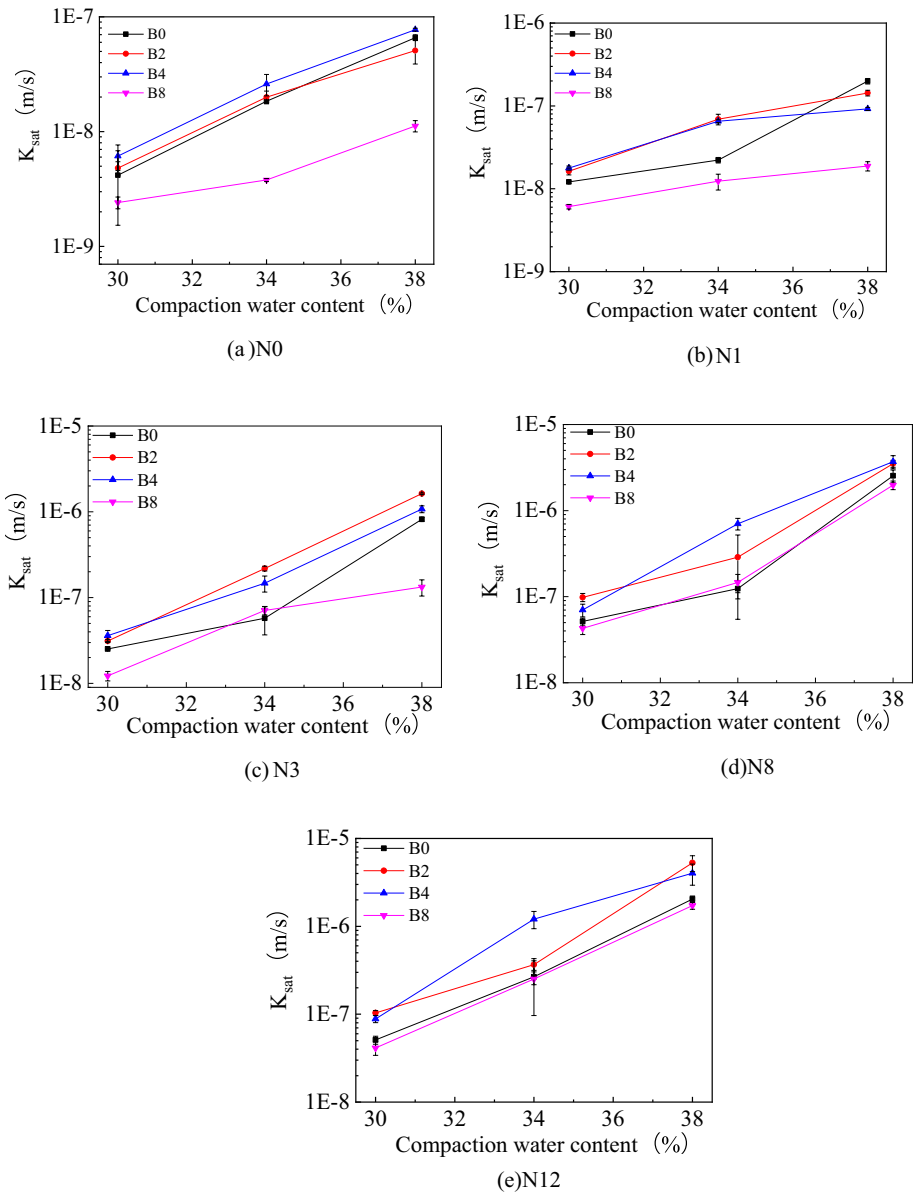

Fig. 10 Influence of compaction water content on saturated permeability at freezing–thawing cycles of **a** N0, **b** N1, **c** N3, **d** N8, **e** N12. (N0, N1, N3, N8, N12 represents the number of freezing–thawing cycle). Experimental data points are presented in mean ± standard deviation (SD). SD of each point of K_{sat} is shown by an error bar

maintain the balance. During the migration of water from unfrozen zone to frozen zone, the clay structure may be rearranged (Fig. 9), resulting in an increase of BAC pores and hence the increase of K_{sat}. This also indicated that the phase change between water and ice in BACs determines the structure change and the variation of permeability of the BAC. Note that in some cases more ice in BAC is difficult to form due to high compaction degree of BAC. Thus the frost heave force can damage the BAC structure and result in a higher void ratio and hence higher K_{sat}. Results from this study indicated that lower compaction water content (i.e., 30%) combining with the higher biochar application rate (i.e., 8%) is suggested to minimize the K_{sat} of BAC used for the field soils forming soil systems in cold regions.

Conclusions

A series of laboratory permeability tests were conducted at compacted clay specimens amended with different application rates of biochar after experiencing cyclic freezing–thawing process. Microstructure and statistical analyses were performed to explain the observed BAC characteristics under freezing–thawing conditions. The following conclusions may be drawn from this study.

1. The results indicated that compaction water content has the most influencing effect on K_{sat} among the three influencing factors ($F = 428.210$, $p = 0.000$). The higher the compaction water content, the higher the K_{sat} would be. This is due to the liquid water migration from unfrozen zone to frozen zone during freezing process, resulting in the redistribution of BAC particles and the increase of BAC pore volume.
2. The number of freezing–thawing cycles was found to be the second most important factor ($F = 152.899$, $p = 0.000$) that would cause an increase in K_{sat}. After freezing–thawing cycles, the K_{sat} of biochar-amended clay was increased by 1 ~ 2 orders of magnitude (i.e., $p < 0.05$). The main reason is that the cyclic freezing–thawing process causes a damage to the BAC structure and generates a large number of micro-cracks in BAC specimens.
3. Increase in the saturated permeability of biochar-amended clay in the first three cycles of freezing–thawing is larger than that of following cycles. This indicates the effect of freezing–thawing to the BAC structure is reduced after three cycles.
4. The application rate of biochar can also affect the K_{sat}, although its effect are less than the above factors ($F = 32.744$, $p = 0.000$). Increase in the saturated permeability due to application of biochar is not stereotypical. Lower biochar application rate (i.e., 0 ~ 4%) increases the saturated permeability of biochar-amended clay, whereas higher biochar application rate (i.e., 4 ~ 8%) causes a reduction. This is attributed to the increase of filled pores of biochar-amended clay resulting from fine particles of clay and micro-particles of biochar driven by the flowing liquid water in the freezing–thawing process. It should be noted that our findings and conclusions are drawn based on the observation for application rates ranged from 0 to 8%, any effects of higher biochar application rates on the findings need to be further investigated in the future. Furthermore, as compared with the K_{sat} of BAC, unsaturated permeability of BAC under cyclic freezing–thawing process is more relevant to the field soil. Therefore, it is necessary to conduct relevant research on this aspect in the future.

Acknowledgements The authors acknowledge the grants (No. 51808171 and No. 52261160382) provided by the National Natural Science Foundation of China and also the grants (CRF/C6006-20G, N_HKUST603/22 and 16202720) provided by the Hong Kong Research Grants Council. The second author (V. Kamchoom) acknowledges the grant (FRB66065/0258-RE-KRIS/FF66/53) from King Mongkut's Institute of Technology Ladkrabang (KMITL) and National Science, Research and Innovation Fund (NSRF), the grant (N10A650844) under Climate Change and Climate Variability Research in Monsoon Asia (CMON3) from the National Research Council of Thailand (NRCT) and the National Natural Science Foundation of China (NSFC).

Authors' contributions ZC: Conceptualization, formal analysis, funding acquisition, investigation, methodology, writing – original draft. VK: Investigation, methodology, writing – review & editing. Anthony Leung: Investigation, writing – review & editing. JX: Data curation, visualization, methodology. RC: Formal analysis, methodology, funding acquisition, supervision, writing – review & editing.

Declarations

Conflict of interest The author declares no competing interests.

Ethical approval Not applicable.

References

Al-Wabel MI, Hussain Q, Usman ARA, Ahmad M, Abduljabbar A, Sallam AS, Ok YS (2017) Impact of biochar properties on soil conditions and agricultural sustainability: a review. Land Degrad Dev 29(7):2124–2161

Andersland O B, Anderson D M (1978) Geotechnical engineering for cold regions McGraw-Hill book co. Inc, New York, N. Y

ASTM C1202 (2006) Standard test method for electrical indication of concrete's ability to resist chloride ion penetration. West Conshohocken, PA: American Society for Testing Materials

ASTM D6035/D6035M-13 (2013) Standard test method for determining the effect of freeze-thaw on permeability of compacted or intact soil specimens using a flexible wall permeameter

Azmatch TF, Sego DC, Arenson LU, Biggar KW (2012) New ice lens initiation condition for frost heave in fine-grained soils. Cold Reg Sci Technol 82:8–13

Barnes RT, Gallagher ME, Masiello CA, Liu Z, Dugan B (2014) Biochar-induced changes in soil permeability and dissolved nutrient fluxes constrained by laboratory experiments. PLoS ONE 9:e108340

Bordoloi S, Gopal P, Boddu R, Wang QH, Cheng YF, Garg A, Sreedeep S (2019) Soil-biochar-water interactions: role of biochar from Eichhornia crassipes in influencing crack propagation and suction in unsaturated soils. J Clean Prod 210:847–859

Brockhoff SR, Christians NE, Killorn RJ, Horton R, Davis DD (2010) Physical and mineral-nutrition properties of sand-based turfgrass root zones amended with biochar. Agron J 102:1627–1631

Chen XW, Wong JTF, Ng CWW, Wong MH (2016) Feasibility of biochar application on a landfill final cover-a review on balancing ecology and shallow slope stability. Environ Sci Pollut Res 23:7111–7125

Chen ZK, Chen CW, Kamchoom V, Chen R (2020) Gas permeability and water retention of a repacked silty sand amended with different particle sizes of peanut shell biochar. Soil Sci Soc Am J 84(5):1630–1641

Chen R, Huang JW, Zhou C, Ping Y, Chen ZK (2021) A new simple and low-cost air permeameter for unsaturated soils. Soil Tillage Res 213:105083

Chen ZK, Kamchoom V, Apriyono A, Chen R, Chen CW (2022) Laboratory study of water infiltration and evaporation in biochar-amended landfill covers under extreme climate. Waste Manag 153:323–334

Chen B, Cai W, Garg A (2023a) Relationship between bioelectricity and soil–water characteristics of biochar-aided plant microbial fuel cell. Acta Geotech J. 12:1–4

Chen R, Huang JW, Leung AK, Chen ZK, Ping Y, Xu Y (2023b) Modelling air conductivity function of unsaturated root-permeated soil. Soil Tillage Res 227:105583

Chiu CF, Huang ZD (2020) Microbial methane oxidation and gas adsorption capacities of biochar-modified soils. Int J Geosynth Groun Eng 6:24

Dong XQ, Chen RF (2017) Research progress of soil properties under freezing and thawing cycles. J Taiyuan Univ Technol 48:275–287

Fu Q, Zhao H, Li TX, Hou RJ, Liu D, Ji Y, Zhou ZQ, Yang LY (2019) Effects of biochar addition on soil hydraulic properties before and after freezing-thawing. CATENA 176:112–124

Garg A, Huang H, Cai W, Reddy NG, Chen P, Han Y, Kamchoom V, Gaurav S, Zhu HH (2021) Influence of soil density on gas permeability and water retention in soils amended with in-house produced biochar. J Rock Mech Geotech Eng 13:593–602

Garg A, Wani I, Zhu H, Kushvaha V (2022) Exploring efficiency of biochar in enhancing water retention in soils with varying grain size distributions using ANN technique. Acta Geotech j 17:1315–1326

Githinji L (2014) Effect of biochar application rate on soil physical and hydraulic properties of a sandy loam. Arch Agron Soil Sci 60:457–470

Gu Q, Wang JD, Si DD, Xu YJ, Ceng P, Li B (2016) Effect of freeze-thaw cycles on collapsibility of loess under different moisture contents. Chin J Geotech Eng 7:1187–1192

Huang H, Reddy NG, Huang X, Chen P, Wang P, Zhang Y, Huang Y, Lin P, Garg A (2021) Effects of pyrolysis temperature, feedstock type and compaction on water retention of biochar amended soil. Sci Rep 11(1):7419

Hussain R, Garg A, Ravi K (2020) Soil-biochar-plant interaction: differences from the perspective of engineered and agricultural soils. Bull Eng Geol Environ 79:4461–4481

Kalkan E, Yarbaşı N, Özgür B, Karimdoust S (2022) Effects of quartzite on the freeze–thaw resistance of clayey soil material from Erzurum. NE Turkey Bull Eng Geol Environ 81:191

Lehmann J, Joseph SM (2009) biochar for environmental management: science and technology. Routledge, New York, U.S.A.

Lim TJ, Spokas KA, Feyereisen G, Novak JM (2016) Predicting the impact of biochar additions on soil hydraulic properties. Chemosphere 142:136–144

Liu ZL, Dugan B, Masiello CA, Wahab LM, Gonnermann HM, Nittrouer JA (2018) Effect of freeze-thaw cycling on grain size of biochar. PLoS ONE 13:e0191246

Ma H (2014) Mercury intrusion porosimetry in concrete technology: tips in measurement, pore structure parameter acquisition and application. J Porous Mat 21:207–215

Othman MA, Benson CH (1993) Effect of freeze-thaw on the permeability and morphology of compacted clay. Can Geotech J 30:236–246

Palmer BG, Edil TB, Benson CH (2000) Liners for waste containment constructed with class F and class C fly ashes. J Hazard Mater 76:193–216

Shibi T, Kamei T (2014) Effect of freeze-thaw cycles on the strength and physical properties of cement-stabilised soil containing recycled basanite and coal ash, Cold Reg. Sci Technol 106:36–45

Tang YQ, Yan JJ (2015) Effect of freeze-thaw on permeability and microstructure of soft soil in Shanghai area. Environ Earth Sci 73:7679–7690

Uzoma KC, Inoue M, Andry H, Fujimaki H, Zahoor A, Nishihara E (2011) Effect of cow manure biochar on maize productivity under sandy soil condition. Soil Use Manag 27:205–212

Wang H, Chen R, Leung AK, Huang JW (2023) Temperature effects on the hydraulic properties of unsaturated rooted soils. Can Geotech J 60(6):1

Wong JTF, Chen ZK, Chen XW, Ng CWW, Wong MH (2017) Soil-water retention behavior of compacted biochar-amended clay: a novel landfill cover material. J Soil Sediment 17:590–598

Wong JTF, Chen ZK, Wong AYY, Ng CWW, Wong MH (2018) Effects of biochar on permeability of compacted kaolin clay. Environ Pollut 234:468–472

Zhao GT, Han Z, Zou WL, Wang XQ (2021) Evolution of mechanical behaviours of an expansive soil during drying-wetting, freeze–thaw, and drying-wetting-freeze–thaw cycles. Bull Eng Geol Environ 80:8109–8121